Original Article

Presentation of a matrix-based method to calculate dose distribution in brachytherapy with photon-emitting sources

Mahdi Ghorbani, Azam Mozaffari, Hossein Akbari-Lalimi

Department of Medical Physics, Faculty of Medicine, Mashhad University of Medical Sciences, Mashhad, Iran

For correspondence:
Azam Mozaffari, Department of Medical Physics, Faculty of Medicine, Mashhad University of Medical Sciences, Pardise Daneshgah, Azadi Square, Mashhad, Iran.
E-mail: mozaffariazam@yahoo.com

ABSTRACT

Aim of Study: The report of the task group number 43(TG-43) of AAPM has been known as the most common method to obtain the dose distribution around brachytherapy sources. The error caused by independent obtaining and rounding and combinational error caused by algebraic operations of each TG-43 dosimetry parameters increase the total error in the calculation of the dose distribution around the brachytherapy sources. The aim of the present study is to present and evaluate a matrix-based approach for simplifying and reducing calculation errors.

Materials and Methods: In this study, the simulation method with MCNPX code was used to obtain the dose distribution. Four sources were simulated, and the dose matrix around these sources was obtained. Finally, the dose distribution obtained from the matrix-based method was compared with the dose distribution obtained from the method of TG-43 report.

Results: There is little difference between the values obtained from the two methods in some points. Absolute mean differences between the values obtained by these two methods were 1.4% for the ^{60}Co, 3.52% for the ^{137}Cs, 2.67% for the ^{192}Ir, and 2.42% for the ^{103}Pd sources. The advantage of the matrix-based method is its simple computing process and less computation time.

Conclusion: Considering that the comparison of brachytherapy sources is not raised in calculations of treatment planning systems and also considering the more uncertainty in the calculation of the dose distribution in TG-43 method, it is recommended that dose distribution obtained from matrix-based method be used as input for treatment planning systems.

KEY WORDS: Brachytherapy, dose distribution, matrix-based approach, Monte Carlo simulation, task group number 43 reports

INTRODUCTION

Brachytherapy is a treatment technique in which one or a number of radioactive sources are used for irradiation of malignant tumors in the vicinity of a tumor. By using this method, tumor can be irradiated with a large dose using high dose gradient. In the past, ^{226}Ra source was used for this purpose, but nowadays the use of sources such as ^{103}Pd, ^{125}I, and ^{192}Ir is growing. This technique plays an important role in cancer treatment in different areas of the body including brain, head and neck, prostate, cervix, etc.[1]

Nowadays, brachytherapy sources are widely used for the treatment of malignancies. Providing an accurate method to obtain dose distribution around these sources is of great importance. The report of the task group number 43 (TG-43) of the American Association of Physicists in Medicine has been known as the most common formalism to obtain the dose distribution around brachytherapy sources, and the method proposed in this report is used in many treatment planning systems. According to this report, dose distribution around brachytherapy sources is calculated using different dosimetric factors, which are obtained through measurement or simulation using Monte Carlo codes in a homogeneous phantom.[1,2] In different studies, these parameters have been reported for various sources through both experimental measurements and simulations. Furthermore, in

Submitted: 13-Nov-16
Revised: 12-Jun-17
Accepted: 24-Feb-18
Published: 24-Dec-19

Access this article online
Website: www.cancerjournal.net
DOI: 10.4103/jcrt.JCRT_1274_16
Quick Response Code:

Cite this article as: Ghorbani M, Mozaffari A, Akbari-Lalimi H. Presentation of a matrix-based method to calculate dose distribution in brachytherapy with photon-emitting sources. J Can Res Ther 2019;15:1245-53.

several published articles, some cases have been expressed as defects of this report.[3-8] Some of these defects include not considering different tissue heterogeneities, disregarding the effect of phantom dimension on dosimetric parameters. Furthermore, the impact of voxel size and capsule material on dosimetric parameters were studied in several research studies.[3-8]

In a point/counterpoint article, the necessity of TG-43 factorization in the calculation of brachytherapy dose distribution is debated.[9] This article suggested that TG-43 method can be replaced with dose rate tables; however, it also indicates the advantages of TG-43 formalism versus dose rate table method. Actually, dose rate tables are produced from multiplying TG-43 parameters such as dose rate constant, geometry factor, anisotropy function, and radial dose function. Eventually, a normalized dose rate table with the dose rate constant can be better and simpler from TG-43 protocol in dose calculation for common brachytherapy sources. Although that article has discussed advantages and disadvantages of TG-43 dose calculation formalism versus direct calculation of dose rate table, it lacks a quantitative comparison of the results of these two methods.

Additional to the mentioned defects in the report of the TG-43, the uncertainty of independent obtaining and rounding, and the combined uncertainty of algebraic operations of dosimetric parameters increase the total uncertainty in the calculation of dose distribution around brachytherapy sources. The aim of this study is to present and evaluate a matrix-based method to calculate dose distribution for photon-emitting brachytherapy sources. It is aimed to present a simpler method with less uncertainty for calculation of dose distribution. In this method, the dose distribution is directly calculated through Monte Carlo simulations, and it avoids the discrepancies related to independent obtaining and rounding of dosimetric parameters and combination of uncertainties.

MATERIALS AND METHODS

Two-dimensional dose distribution around four brachytherapy sources (^{60}Co, ^{137}Cs, ^{192}Ir, and ^{103}Pd) was obtained through two methods. The use of simulation of the sources and direct obtaining the dose distribution was considered as the first method and obtaining the dose distribution using TG-43 protocol was the second method. The first method was presented as the proposed method of this study. Finally, validation and evaluation of the matrix-based method were conducted through comparing the results of dose distributions from the two methods.

Geometry of sources

In this study, four brachytherapy sources were simulated: ^{60}Co BEBIG (model Co0.A86), ^{137}Cs (model 67–6520) Isotope Product Laboratories (IPL, Valencia, CA), ^{192}Ir (model BEBIG), and ^{103}Pd (model OptiSeed). The simulations were performed using MCNPX (version 2.4.0) Monte Carlo code (Los Alamos National Laboratory, Los Alamos, New Mexico, United States). The geometry of these sources is shown in Figure 1.

The model of the ^{60}Co source studied in this study is Co0.A86. As it can be seen from Figure 1a, this source is formed from a central cylindrical shape core containing ^{60}Co with a length of 3.5 mm and a diameter of 0.5 mm. The central core is located inside a cylindrical capsule with inner diameter of 0.7 mm and outer diameter of 1 mm. The length of the cable of this source is 5 mm.[10]

A ^{137}Cs source, model 67–6520, was evaluated. As it is shown in Figure 1b, the active core of this source is a cylinder with length of 14.8 mm and diameter of 1.52 mm. The core of this source contains radioactive cesium oxide. The density of this material is 1.47 g/cm^3. This core is located inside a stainless steel capsule with density of 7.9 g/cm^3.[11]

Based on Figure 1c, the ^{192}Ir source (model BEBIG) contains a central radioactive core with length of 3.5 mm and diameter of 0.6 mm containing ^{192}Ir. This part is located inside a stainless steel capsule with density of 7.8 g/cm^3 with diameter of 1 mm and length of 5 mm. The cable of this source is made of stainless steel with length of 6 mm and diameter of 1 mm.[12]

The ^{103}Pd source (model OptiSeed) is shown in Figure 1d. This source has two active cores with length of 0.7 mm and diameter of 0.4 mm. A goldmarker with length of 2 mm and diameter of 0.4 mm is located in the central part.[3]

Validation of source simulations

The validation of simulation of the sources was performed in a previous study in this field.[13] In that study, TG-43 parameters of the sources were calculated and were compared with other corresponding studies. The parameters included dose rate constant, radial dose function, and anisotropy function for the ^{60}Co, ^{137}Cs, ^{192}Ir, and ^{103}Pd sources. The results of comparisons showed good agreement with the other studies. For example, dose rate constant differences for the ^{60}Co, ^{137}Cs, ^{192}Ir, and ^{103}Pd sources were 3.04%, 3.39%, 0.53%, and 0.68%, respectively. Based on the agreement between the results of that study and the other studies, the TG-43 dosimetric parameter calculation for the ^{60}Co (Co0.A86), ^{137}Cs (67–65200), ^{192}Ir (BEBIG), and ^{103}Pd (OptiSeed) sources were validated.

Moreover, to obtain two-dimensional dose distribution with TG43 method, the dosimetric parameters obtained in that study were used in the present study. These parameters include air kerma strength, dose rate constant, radial dose function, and anisotropy function.

Dose distribution by matrix-based method

The energy spectrum for ^{60}Co source had the energies of 1.33 and 1.17 MeV with probability of 50% for each of them. The energy spectra of ^{137}Cs, ^{192}Ir, and ^{103}Pd sources are listed in Table 1.

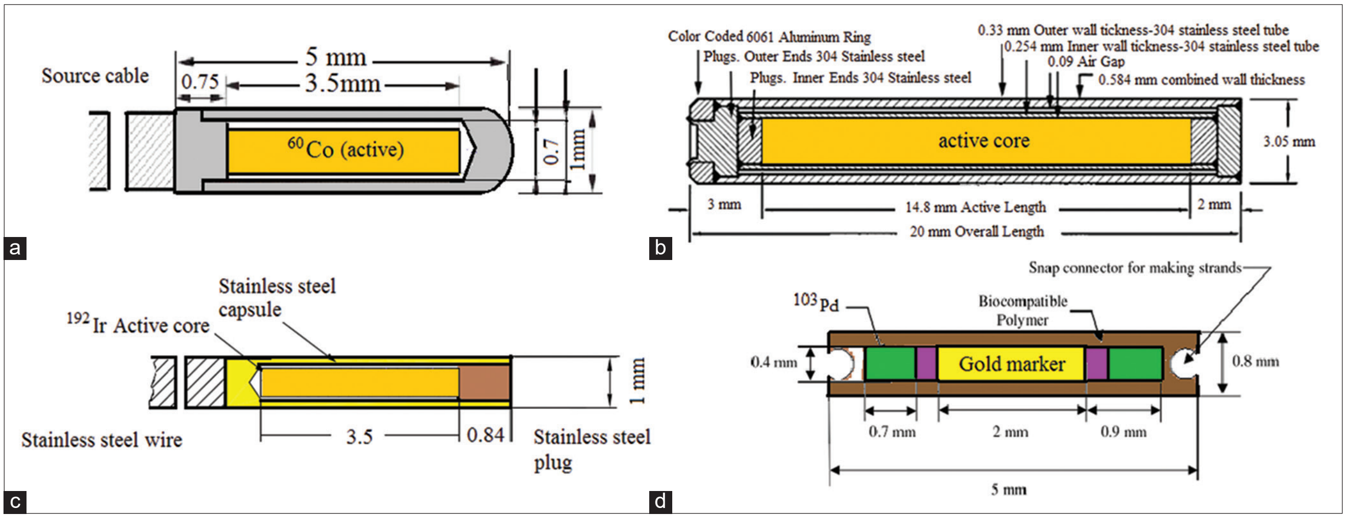

Figure 1: Geometry of (a) 60Co (model Co0.A86), (b) 137Cs (model 67-6520), (c) 192Ir (model BEBIG), and (d) 103Pd (model OptiSeed) sources used in the presented study

Table 1: Energy spectrum of ^{137}Cs, ^{192}Ir, and ^{103}Pd sources

^{137}Cs		^{192}Ir		^{103}Pd	
Energy (keV)	Intensity (%)	Energy (keV)	Intensity (%)	Energy (keV)	Intensity (%)
4.47	0.914	9.44	3.9216	2.7	8.7321
31.817	1.995	65.122	2.626	20.074	22.47
32.194	3.641	66.831	4.441	20.216	42.512
36.304	0.3489	75.368	0.53111	22.699	3.541
36.378	0.67218	75.749	1.02122	22.724	6.8519
37.255	0.2136	77.831	0.3648	23.172	1.645
283.51	0.00059	136.393	0.19925	39.7488	0.0683
661.6573	85.102	176.984	0.00431	53.291	3.0×10^{-5}
		280.2724	0.0084	62.413	0.001044
		295.9565	28.72	241.885	5.0×10^{-7}
		308.45507	29.707	294.9815	0.002807
		316.50618	82.86	317.725	1.5×10^{-5}
		416.46887	0.67021	357.458	0.02217
		468.06885	47.843	443.795	1.5×10^{-5}
		485.456	0.00474	497.0801	0.003961
		588.58107	4.5221		
		593.6319	0.04201		
		599.4115	0.003917		
		604.41105	8.21619		
		612.46215	5.347		
		765.83	0.00136		
		884.53657	0.2927		
		1061.494	0.05316		
		1089.9626	0.0011616		
		1378.5024	0.0014019		

To calculate the dose distribution around the sources, each source was defined at the center of a spherical water phantom with radius of 200 cm. Voxels with dimensions of 1 mm × 1 mm × 1 mm on *Y-Z* plane in the range of −14 cm to 14 cm in the direction of *Z*-axis and in the range of 0 cm to 14 cm in the direction of *Y*-axis were selected for the ^{60}Co, ^{137}Cs, and ^{192}Ir sources. Voxel of the same size on *Y-Z* plane in the range of 0 cm to 5 cm in the direction of *Y* and *Z* axes was considered for the ^{103}Pd source. With this regard, the *Z* axis is located on the longitudinal axis of the source. In these programs, the type 1 mesh tally with "pedep" option was used. Energy cutoff for photons and electrons was 10 keV for the ^{60}Co and ^{137}Cs sources. This value was considered as 5 and 1 keV for the ^{192}Ir and ^{103}Pd sources, respectively. The number of tracked particles in all programs was 10^9 histories. The mesh tally was used in this scoring and tracking more histories could result in a long time for the simulation. The maximum statistical uncertainty in Monte Carlo calculations obtained for the ^{60}Co, ^{137}Cs, ^{192}Ir, and ^{103}Pd sources was 2.3%, 2.1%, 2.4% and 5.4%, respectively. This statistical uncertainties are relatively low; however, they could have minor effect on dose distribution results. The output files obtained from running these programs were transferred into Microsoft Excel software and then were converted to matrixes with 281 × 281 voxels using MATLAB software for processing the data for the ^{60}Co, ^{137}Cs, and ^{192}Ir sources. In the case of the ^{103}Pd source, the data were converted into a matrix with dimensions of 101 × 101 voxels using MATLAB software. To compare the two-dimensional dose distribution obtained by two methods (matrix based and TG-43) for the ^{60}Co, ^{137}Cs, ^{192}Ir, and ^{103}Pd sources, the required rows and columns of these matrixes were extracted. In this section, according to the data obtained from the output file from the tally calculations, the average energy deposited per unit volume in each mesh cell is regarding MeV/cm^3 per photon and it must be converted to absorbed dose rate in each mesh cell regarding cGy/(h.U). Therefore, to obtain the absorbed dose rate, the amount of photon yield and activity per air kerma strength was introduced for each source. For the ^{60}Co, ^{137}Cs, ^{192}Ir, and ^{103}Pd sources, the photon yield was 2.00, 0.929, 2.214, and 0.859 (photons/dis), respectively. The amount of activity per unit air kerma strength was $\frac{1}{3.029\times10^{-7}}(\mathrm{Bq/U})$, $\frac{1}{7.61\times10^{-8}}(\mathrm{Bq/U})$, $\frac{1}{9.483\times10^{-8}}(\mathrm{Bq/U})$ and $\frac{1}{3.27\times10^{-8}}(\mathrm{Bq/U})$ for these sources, respectively.

However, it should be noticed that the activity of sources has no application according to TG-43 report and the strength of a source is described on the basis of air kerma strength. In the above conversions, the sources' activities were only used for conversion of the units, and these conversion factors were obtained by having relation between the output programs of air kerma strength and dose rate.

Dose distribution by task group number 43 method

For comparison of dose rate obtained by the two mentioned methods, certain points in Cartesian space, in which the dose rates were obtained through matrix-based method were selected. To obtain the dose rate values in the Cartesian space with TG-43 method, it was required to convert the data in the polar space (r, θ) to the data in the Cartesian space. There were a large number of specific points in the Cartesian space which had no corresponding TG-43 parameters. To calculate the dose rate for these points, the neighborhood points of these points in which the TG-43 parameters were specified, were used. To calculate the dose rate at these points, from the TG-43 parameters at the neighborhood points, adequate interpolations were performed. For obtaining the dose rate at the desired points from the corresponding TG-43 parameters and for interpolation of the TG-43 dosimetric parameters MATLAB software was used.

To estimate the dose, at the desired points for comparison of dose distributions from TG-43 formalism, using the calculated dose by TG-43 formalism in the neighborhood points, three different modes were possible:

- TG-43 guideline parameters at the desired point of comparison have been obtained through simulation, that in this case, the use of the neighborhood points is not needed and the parameters relating to this point were used to obtain the dose
- The desired point of comparison is located on the line connecting two points where TG-43 parameters have been obtained. In this case, to estimate the dose of desired point, TG-43 parameters of these points were interpolated by these parameters for these two mentioned points. Interpolations were performed based on the amount of TG-43 parameters for two mentioned points, and the distance of these points from the desired point of comparison. In other words, TG-43 parameters for these points were calculated by linear interpolation
- The desired point of comparison is in an area between four points, in which TG-43 parameters have been obtained. In this case, to estimate the dose of desired point, TG-43 parameters of this point was interpolated by TG-43 parameters from the four mentioned points. Like the previous case, interpolations were performed based on the values of TG-43 parameters at the four mentioned points and the distance of each point from the desired point of comparison. Actually, for these points, bilinear interpolation was applied. Bilinear interpolation is a nonlinear interpolation that consists of two linear interpolations. In this case, one linear interpolation was regarding radial distance, and the other was regarding polar angle. Deviation of dose from linearity in polar and radial directions can add dosimetric error of this interpolation and on the other hand, since this method results in weighted averages it can decrease the fluctuations in the dose data.

RESULTS

In this section, the results of two-dimensional dose distribution obtained from matrix-based method and dose distribution obtained from TG-43 method are presented. In addition, the percentage differences between these two methods are provided for the ^{60}Co, ^{137}Cs, ^{192}Ir, and ^{103}Pdsources.

The results of dose distribution obtained from matrix-based and TG-43 methods for ^{60}Co source are presented in Tables 2 and 3, respectively.

The results of dose distribution obtained from matrix-based and TG-43 methods for ^{137}Cs source are presented in Tables 4 and 5, respectively.

The results of dose distribution obtained from matrix-based and TG-43 methods for ^{192}Ir source are presented in Tables 6 and 7, respectively.

The results of dose distribution obtained from matrix-based and TG-43 methods for ^{103}Pd source are presented in Tables 8 and 9, respectively.

DISCUSSION

In this study, ^{60}Co, ^{137}Cs, ^{192}Ir, and ^{103}Pd brachytherapy sources were simulated and dose distribution around these sources was calculated using matrix-based method. To evaluate the methodology presented in this study, a comparison was performed between the results of dose distribution obtained from the matrix-based method, and the results of dose distribution obtained from TG-43 method. In comparison of the dose distribution obtained from the matrix-based approach and TG-43 method in this study, the maximum percentage difference between the values obtained from these two methods for the ^{60}Co source was 8.55%. The average of absolute of percentage difference between these methods for this source was 1.40%.

The comparison of the dose distribution obtained for the ^{137}Cs source in the study using the matrix-based approach and TG-43 method is performed. The maximum percentage difference was obtained as 10.18%, and the average of absolute of difference percentage was obtained equal to 3.52%. For this source, relatively large differences between the two methods were also observed in some points, especially for those points that are farthest from the source. It seems that these differences

Table 2: Two-dimensional dose distribution per air kerma strength (cGy/h/U) for ^{60}Co source obtained from the matrix-based method

Z (cm)	*Y* (cm)												
	0	0.5	1	1.5	2	2.5	3	4	5	6	8	10	14
−14	0.00384	0.00382	0.00405	0.00384	0.00391	0.00397	0.00389	0.00379	0.00365	0.00350	0.00297	0.00253	0.00169
−10	0.00833	0.00845	0.00852	0.00861	0.00882	0.00843	0.00836	0.00792	0.00736	0.00666	0.00522	0.00417	0.00260
−8	0.01339	0.01371	0.01415	0.01432	0.01375	0.01340	0.01315	0.01181	0.01050	0.00926	0.00701	0.00532	0.00301
−6	0.02440	0.02541	0.02594	0.02528	0.02446	0.02346	0.02216	0.01890	0.01606	0.01335	0.00931	0.00650	0.00348
−5	0.03559	0.03748	0.03803	0.03662	0.03492	0.03231	0.02957	0.02423	0.01978	0.01588	0.01068	0.00721	0.00371
−4	0.05711	0.06037	0.05920	0.05640	0.05140	0.04636	0.04107	0.03172	0.02445	0.01877	0.01188	0.00799	0.00386
−3	0.10203	0.10931	0.10374	0.09323	0.08006	0.06813	0.05813	0.04089	0.02956	0.02221	0.01311	0.00853	0.00404
−2.5	0.14814	0.15845	0.14578	0.12424	0.10270	0.08435	0.06836	0.04644	0.03253	0.02351	0.01355	0.00892	0.00406
−2	0.23347	0.24635	0.21310	0.17025	0.13343	0.10322	0.08009	0.05166	0.03524	0.02487	0.01437	0.00906	0.00408
−1.5	0.42038	0.42994	0.33178	0.23968	0.17127	0.12535	0.09380	0.05726	0.03757	0.02626	0.01430	0.00913	0.00422
−1	0.97400	0.88041	0.54542	0.33161	0.21374	0.14755	0.10588	0.06108	0.03928	0.02697	0.01498	0.00925	0.00419
−0.5	-	2.23862	0.87300	0.43253	0.25252	0.16371	0.11339	0.06405	0.04049	0.02781	0.01505	0.00933	0.00422
0	-	4.26573	1.08453	0.48095	0.26919	0.17035	0.11746	0.06522	0.04083	0.02819	0.01533	0.00943	0.00436
0.5	4.81914	2.24011	0.87074	0.43170	0.25303	0.16470	0.11490	0.06438	0.04069	0.02794	0.01521	0.00924	0.00419
1	1.06755	0.88160	0.54367	0.33239	0.21414	0.14715	0.10557	0.06088	0.03959	0.02731	0.01488	0.00918	0.00421
1.5	0.46083	0.43063	0.33264	0.23838	0.17081	0.12435	0.09381	0.05688	0.03784	0.02646	0.01460	0.00919	0.00421
2	0.25611	0.24801	0.21408	0.17025	0.13310	0.10331	0.08044	0.05186	0.03525	0.02458	0.01443	0.00895	0.00430
2.5	0.16198	0.15985	0.14496	0.12339	0.10296	0.08385	0.06864	0.04624	0.03251	0.02352	0.01383	0.00874	0.00413
3	0.11129	0.11102	0.10461	0.09385	0.08032	0.06856	0.05754	0.04109	0.02995	0.02223	0.01312	0.00840	0.00404
4	0.06185	0.06156	0.06009	0.05591	0.05173	0.04604	0.04088	0.03166	0.02423	0.01877	0.01190	0.00795	0.00381
5	0.03908	0.03867	0.03828	0.03700	0.03445	0.03239	0.02967	0.02418	0.01970	0.01584	0.01060	0.00716	0.00360
6	0.02674	0.02651	0.02659	0.02578	0.02468	0.02333	0.02207	0.01879	0.01604	0.01333	0.00939	0.00669	0.00345
8	0.01454	0.01455	0.01427	0.01416	0.01399	0.01342	0.01289	0.01197	0.01057	0.00914	0.00709	0.00533	0.00296
10	0.00891	0.00890	0.00880	0.00884	0.00875	0.00859	0.00832	0.00790	0.00722	0.00672	0.00521	0.00436	0.00258
14	0.00401	0.00415	0.00428	0.00398	0.00394	0.00402	0.00388	0.00386	0.00371	0.00336	0.00289	0.00255	0.00179

Table 3: Two-dimensional dose distribution per air kerma strength (cGy/h/U) for ^{60}Co source obtained from the task group number-43 method

Z (cm)	*Y* (cm)												
	0	0.5	1	1.5	2	2.5	3	4	5	6	8	10	14
−14	0.00379	0.00396	0.00401	0.00404	0.00403	0.00401	0.00397	0.00385	0.00368	0.00348	0.00304	0.00260	0.00183
−10	0.00783	0.00845	0.00863	0.00857	0.00852	0.00847	0.00827	0.00773	0.00716	0.00652	0.00532	0.00420	0.00262
−8	0.01294	0.01356	0.01379	0.01372	0.01360	0.01321	0.01268	0.01159	0.01038	0.00924	0.00706	0.00531	0.00307
−6	0.02434	0.02557	0.02591	0.02561	0.02463	0.02338	0.02199	0.01889	0.01576	0.01314	0.00925	0.00660	0.00353
−5	0.03363	0.03719	0.03766	0.03649	0.03435	0.03202	0.02955	0.02451	0.01995	0.01576	0.01047	0.00724	0.00374
−4	0.05646	0.06062	0.06017	0.05628	0.05126	0.04611	0.04064	0.03162	0.02452	0.01903	0.01172	0.00785	0.00393
−3	0.10034	0.10627	0.10214	0.09164	0.08026	0.06870	0.05797	0.04079	0.02981	0.02226	0.01287	0.00840	0.00408
−2.5	0.14971	0.15742	0.14366	0.12180	0.10101	0.08343	0.06901	0.04638	0.03247	0.02371	0.01342	0.00865	0.00415
−2	0.24247	0.25119	0.21489	0.17020	0.13052	0.10126	0.08059	0.05197	0.03499	0.02507	0.01391	0.00886	0.00421
−1.5	0.42780	0.42962	0.33603	0.24266	0.17086	0.12248	0.09271	0.05720	0.03729	0.02629	0.01433	0.00903	0.00426
−1	1.01231	0.89534	0.54812	0.33689	0.21676	0.14560	0.10395	0.06187	0.03916	0.02723	0.01464	0.00916	0.00430
−0.5	-	2.32122	0.89210	0.43298	0.25734	0.16380	0.11233	0.06503	0.04036	0.02785	0.01485	0.00924	0.00432
0	-	4.34303	1.12000	0.47995	0.27446	0.17070	0.11504	0.06601	0.04076	0.02808	0.01493	0.00927	0.00434
0.5	4.88399	2.31649	0.88953	0.43315	0.25731	0.16372	0.11216	0.06490	0.04037	0.02789	0.01483	0.00923	0.00433
1	1.08467	0.90233	0.54672	0.33610	0.21651	0.14544	0.10388	0.06181	0.03922	0.02732	0.01462	0.00914	0.00430
1.5	0.45139	0.43077	0.33680	0.24300	0.17052	0.12226	0.09250	0.05727	0.03744	0.02641	0.01431	0.00901	0.00427
2	0.25758	0.25294	0.21543	0.17099	0.13076	0.10111	0.08032	0.05174	0.03509	0.02524	0.01395	0.00884	0.00422
2.5	0.16166	0.16001	0.14356	0.12229	0.10152	0.08362	0.06888	0.04604	0.03237	0.02382	0.01351	0.00865	0.00416
3	0.11012	0.10941	0.10204	0.09177	0.08046	0.06916	0.05809	0.04069	0.02963	0.02226	0.01299	0.00842	0.00409
4	0.06483	0.06313	0.06055	0.05634	0.05130	0.04609	0.04064	0.03162	0.02452	0.01899	0.01173	0.00787	0.00393
5	0.04064	0.03907	0.03846	0.03665	0.03445	0.03204	0.02963	0.02445	0.01988	0.01573	0.01046	0.00724	0.00374
6	0.02681	0.02666	0.02663	0.02576	0.02472	0.02339	0.02197	0.01895	0.01568	0.01309	0.00925	0.00659	0.00353
8	0.01418	0.01411	0.01422	0.01401	0.01366	0.01323	0.01272	0.01158	0.01042	0.00920	0.00703	0.00531	0.00308
10	0.00898	0.00872	0.00878	0.00876	0.00866	0.00851	0.00828	0.00775	0.00715	0.00655	0.00529	0.00420	0.00262
14	0.00402	0.00407	0.00411	0.00412	0.00411	0.00406	0.00399	0.00384	0.00368	0.00348	0.00305	0.00261	0.00184

are due to the related uncertainties in the calculation of TG-43 parameters and their combined uncertainties.

The comparison of the dose distribution obtained using the matrix-based approach, and TG-43 method has a maximum percentage difference of 26.6% and the average of absolute of percentage difference of 2.67%. The dose values obtained from these two methods for the ^{192}Ir source revealed good agreement with each other in many points. The difference between these two methods was observed at distances far from the source.

Table 4: Two-dimensional dose distribution per air kerma strength (cGy/h/U) for ^{137}Cs source obtained from the matrix-based method

Z (cm)	*Y* (cm)												
	0	0.5	1	1.5	2	2.5	3	4	5	6	8	10	14
−14	0.00436	0.00420	0.00434	0.00413	0.00417	0.00424	0.00414	0.00401	0.00383	0.00371	0.00319	0.00270	0.00189
−10	0.00923	0.00928	0.00909	0.00899	0.00925	0.00872	0.00870	0.00818	0.00772	0.00688	0.00561	0.00450	0.00274
−8	0.01529	0.01515	0.01458	0.01457	0.01420	0.01398	0.01360	0.01248	0.01131	0.00972	0.00747	0.00554	0.00327
−6	0.02810	0.02709	0.02645	0.02638	0.02580	0.02436	0.02308	0.01999	0.01688	0.01435	0.01008	0.00706	0.00371
−5	0.04124	0.03967	0.03939	0.03837	0.03698	0.03397	0.03158	0.02594	0.02101	0.01705	0.01141	0.00785	0.00400
−4	0.06589	0.06311	0.06249	0.05904	0.05429	0.04908	0.04379	0.03341	0.02607	0.02020	0.01273	0.00853	0.00415
−3	0.12157	0.11604	0.11196	0.09960	0.08558	0.07249	0.06111	0.04350	0.03150	0.02337	0.01417	0.00890	0.00442
−2.5	0.18039	0.17134	0.15882	0.13464	0.11036	0.08933	0.07206	0.04895	0.03397	0.02512	0.01459	0.00944	0.00440
−2	0.30081	0.27990	0.23784	0.18531	0.14167	0.10891	0.08505	0.05465	0.03753	0.02637	0.01499	0.00964	0.00449
−1.5	0.61460	0.53331	0.37726	0.25799	0.18085	0.13065	0.09791	0.05971	0.03947	0.02815	0.01541	0.00984	0.00442
−1	-	1.23094	0.60534	0.34949	0.22184	0.15190	0.10998	0.06421	0.04155	0.02887	0.01577	0.00966	0.00464
−0.5	-	2.52736	0.86758	0.43387	0.25711	0.16848	0.11827	0.06725	0.04280	0.02936	0.01624	0.00980	0.00453
0	-	3.01858	0.98157	0.46797	0.26906	0.17525	0.12168	0.06869	0.04339	0.02964	0.01596	0.00983	0.00460
0.5	-	2.52902	0.86503	0.43270	0.25729	0.16866	0.11839	0.06708	0.04267	0.02941	0.01594	0.00982	0.00454
1	-	1.23187	0.60641	0.34876	0.22223	0.15209	0.10995	0.06422	0.04166	0.02910	0.01606	0.00975	0.00452
1.5	0.62874	0.52968	0.37570	0.25863	0.18120	0.13111	0.09796	0.06016	0.03933	0.02791	0.01542	0.00970	0.00467
2	0.30707	0.28020	0.23845	0.18513	0.14250	0.10921	0.08533	0.05412	0.03723	0.02664	0.01520	0.00941	0.00449
2.5	0.18468	0.17209	0.15913	0.13464	0.10980	0.08954	0.07323	0.04951	0.03427	0.02513	0.01476	0.00928	0.00446
3	0.12372	0.11617	0.11102	0.10028	0.08606	0.07281	0.06084	0.04357	0.03177	0.02331	0.01388	0.00923	0.00439
4	0.06687	0.06359	0.06250	0.05953	0.05475	0.04919	0.04324	0.03359	0.02589	0.02017	0.01251	0.00854	0.00420
5	0.04170	0.04018	0.03957	0.03844	0.03677	0.03402	0.03141	0.02580	0.02109	0.01711	0.01141	0.00768	0.00395
6	0.02835	0.02766	0.02731	0.02677	0.02593	0.02470	0.02312	0.01976	0.01688	0.01426	0.00994	0.00703	0.00377
8	0.01543	0.01495	0.01459	0.01483	0.01462	0.01419	0.01365	0.01258	0.01115	0.00994	0.00768	0.00577	0.00322
10	0.00951	0.00936	0.00923	0.00894	0.00912	0.00896	0.00869	0.00805	0.00749	0.00696	0.00564	0.00457	0.00268
14	0.00432	0.00448	0.00441	0.00415	0.00420	0.00415	0.00421	0.00410	0.00393	0.00368	0.00332	0.00275	0.00191

Table 5: Two-dimensional dose distribution per air kerma strength (cGy/h/U) for ^{137}Cs source obtained from the task group number-43 method

Z (cm)	*Y* (cm)												
	0	0.5	1	1.5	2	2.5	3	4	5	6	8	10	14
−14	0.00425	0.00419	0.00410	0.00405	0.00404	0.00402	0.00398	0.00387	0.00372	0.00353	0.00309	0.00265	0.00188
−10	0.00901	0.00867	0.00859	0.00855	0.00849	0.00844	0.00829	0.00783	0.00724	0.00666	0.00542	0.00430	0.00268
−8	0.01512	0.01443	0.01419	0.01403	0.01399	0.01366	0.01316	0.01190	0.01063	0.00933	0.00719	0.00545	0.00314
−6	0.02880	0.02671	0.02657	0.02589	0.02495	0.02362	0.02204	0.01896	0.01641	0.01374	0.00941	0.00677	0.00361
−5	0.03984	0.03778	0.03756	0.03671	0.03527	0.03306	0.03065	0.02505	0.01984	0.01647	0.01080	0.00741	0.00384
−4	0.06177	0.06158	0.06026	0.05727	0.05228	0.04707	0.04158	0.03283	0.02509	0.01921	0.01223	0.00802	0.00404
−3	0.12292	0.11487	0.10887	0.09717	0.08377	0.07061	0.05911	0.04177	0.03092	0.02250	0.01361	0.00858	0.00421
−2.5	0.17807	0.16669	0.15347	0.13151	0.10805	0.08705	0.07025	0.04702	0.03346	0.02420	0.01420	0.00883	0.00428
−2	0.28737	0.26616	0.22748	0.17925	0.13859	0.10678	0.08294	0.05253	0.03589	0.02578	0.01471	0.00905	0.00433
−1.5	0.59342	0.51123	0.36145	0.24626	0.17471	0.12839	0.09599	0.05776	0.03810	0.02718	0.01512	0.00923	0.00438
−1	-	1.22165	0.58982	0.33455	0.21350	0.14810	0.10779	0.06208	0.03989	0.02828	0.01546	0.00936	0.00441
−0.5	-	2.41947	0.85899	0.41767	0.24480	0.16344	0.11662	0.06491	0.04104	0.02894	0.01569	0.00945	0.00443
0	-	3.07860	0.98000	0.45260	0.25714	0.16867	0.11926	0.06584	0.04145	0.02914	0.01579	0.00949	0.00443
0.5	-	2.43409	0.85895	0.41806	0.24458	0.16336	0.11655	0.06476	0.04100	0.02891	0.01567	0.00944	0.00443
1	-	1.21919	0.58996	0.33411	0.21344	0.14860	0.10811	0.06185	0.03982	0.02824	0.01543	0.00936	0.00441
1.5	0.60939	0.51218	0.36141	0.24665	0.17494	0.12885	0.09614	0.05754	0.03803	0.02714	0.01507	0.00922	0.00437
2	0.29030	0.26819	0.22832	0.17934	0.13880	0.10686	0.08287	0.05240	0.03583	0.02572	0.01463	0.00904	0.00433
2.5	0.18197	0.16813	0.15434	0.13124	0.10809	0.08694	0.07008	0.04690	0.03340	0.02412	0.01410	0.00882	0.00427
3	0.12702	0.11547	0.10947	0.09747	0.08379	0.07036	0.05890	0.04147	0.03085	0.02241	0.01349	0.00857	0.00420
4	0.06943	0.06205	0.06050	0.05719	0.05248	0.04699	0.04160	0.03277	0.02498	0.01908	0.01213	0.00800	0.00404
5	0.04186	0.03906	0.03806	0.03690	0.03532	0.03310	0.03069	0.02510	0.01980	0.01634	0.01071	0.00736	0.00384
6	0.02929	0.02728	0.02654	0.02593	0.02496	0.02360	0.02204	0.01903	0.01645	0.01372	0.00936	0.00671	0.00362
8	0.01522	0.01450	0.01438	0.01423	0.01401	0.01358	0.01305	0.01195	0.01065	0.00938	0.00719	0.00543	0.00315
10	0.00899	0.00865	0.00872	0.00865	0.00855	0.00842	0.00821	0.00775	0.00725	0.00666	0.00542	0.00429	0.00268
14	0.00433	0.00402	0.00408	0.00407	0.00405	0.00403	0.00400	0.00388	0.00368	0.00351	0.00310	0.00267	0.00189

In comparison of the dose distribution obtained from the matrix-based approach and the TG-43 method, the maximum percentage difference for the ^{103}Pd source was 5.03%, and the average of absolute of percentage difference was 2.42%. For this source, differences between the two methods were also observed in some points, especially for the points that are farthest from the source.

In a point/counterpoint article by Song *et al*., the necessity of TG-43 factorization in calculation of brachytherapy dose

Table 6: Two-dimensional dose distribution per air kerma strength (cGy/h/U) for ^{192}Ir source obtained from the matrix-based method

Z (cm)	*Y* (cm)												
	0	0.5	1	1.5	2	2.5	3	4	5	6	8	10	14
−14	0.00344	0.00346	0.00363	0.00355	0.00362	0.00365	0.00370	0.00366	0.00364	0.00337	0.00296	0.00254	0.00154
−10	0.00757	0.00777	0.00793	0.00832	0.00861	0.00840	0.00854	0.00824	0.00758	0.00732	0.00579	0.00464	0.00264
−8	0.01157	0.01196	0.01288	0.01350	0.01346	0.01319	0.01337	0.01236	0.01115	0.01002	0.00772	0.00591	0.00330
−6	0.01962	0.02143	0.02347	0.02411	0.02402	0.02377	0.02262	0.01956	0.01718	0.01441	0.01043	0.00740	0.00367
−5	0.02718	0.03075	0.03421	0.03484	0.03444	0.03266	0.03050	0.02590	0.02138	0.01757	0.01183	0.00821	0.00395
−4	0.04046	0.04903	0.05380	0.05384	0.05104	0.04734	0.04251	0.03383	0.02657	0.02092	0.01326	0.00902	0.00408
−3	0.06811	0.08955	0.09526	0.09068	0.08072	0.07059	0.06070	0.04408	0.03224	0.02427	0.01492	0.00951	0.00426
−2.5	0.09525	0.13188	0.13545	0.12261	0.10477	0.08762	0.07175	0.05001	0.03542	0.02608	0.01543	0.00984	0.00438
−2	0.14392	0.21004	0.20263	0.17037	0.13676	0.10764	0.08545	0.05570	0.03870	0.02779	0.01592	0.01024	0.00440
−1.5	0.24871	0.37868	0.32255	0.24224	0.17686	0.13144	0.09956	0.06180	0.04088	0.02924	0.01620	0.01014	0.00442
−1	0.55859	0.81413	0.54324	0.33904	0.22279	0.15520	0.11239	0.06608	0.04312	0.02997	0.01673	0.01047	0.00443
−0.5	-	2.19480	0.88648	0.44718	0.26283	0.17247	0.12090	0.06938	0.04451	0.03087	0.01692	0.01048	0.00457
0	-	4.31391	1.11004	0.49792	0.28191	0.18007	0.12531	0.07037	0.04512	0.03123	0.01707	0.01055	0.00453
0.5	3.38855	2.19468	0.88457	0.44555	0.26368	0.17377	0.12240	0.06954	0.04466	0.03072	0.01692	0.01043	0.00452
1	0.71997	0.81219	0.54060	0.34012	0.22219	0.15502	0.11231	0.06592	0.04304	0.03044	0.01672	0.01037	0.00449
1.5	0.31438	0.37860	0.32226	0.24105	0.17624	0.13007	0.09917	0.06103	0.04143	0.02925	0.01642	0.01042	0.00457
2	0.17824	0.21054	0.20303	0.16997	0.13599	0.10775	0.08514	0.05609	0.03799	0.02761	0.01608	0.01017	0.00461
2.5	0.11596	0.13365	0.13508	0.12159	0.10391	0.08710	0.07239	0.04984	0.03563	0.02609	0.01543	0.00983	0.00437
3	0.08227	0.09226	0.09581	0.09088	0.08112	0.07050	0.06041	0.04374	0.03252	0.02454	0.01473	0.00939	0.00419
4	0.04718	0.05131	0.05438	0.05369	0.05138	0.04699	0.04233	0.03392	0.02662	0.02070	0.01328	0.00880	0.00408
5	0.03097	0.03324	0.03464	0.03510	0.03393	0.03280	0.03031	0.02571	0.02157	0.01747	0.01183	0.00810	0.00380
6	0.02186	0.02311	0.02400	0.02430	0.02391	0.02333	0.02277	0.01984	0.01727	0.01474	0.01032	0.00755	0.00367
8	0.01282	0.01284	0.01332	0.01345	0.01359	0.01353	0.01330	0.01233	0.01128	0.01001	0.00774	0.00580	0.00314
10	0.00808	0.00814	0.00834	0.00855	0.00840	0.00851	0.00850	0.00815	0.00759	0.00705	0.00578	0.00457	0.00258
14	0.00365	0.00378	0.00380	0.00369	0.00367	0.00367	0.00372	0.00370	0.00348	0.00332	0.00295	0.00260	0.00161

Table 7: Two-dimensional dose distribution per air kerma strength (cGy/h/U) for ^{192}Ir source obtained from the task group number-43 method

Z (cm)	*Y* (cm)												
	0	0.5	1	1.5	2	2.5	3	4	5	6	8	10	14
−14	0.00377	0.00380	0.00392	0.00399	0.00403	0.00405	0.00405	0.00402	0.00390	0.00372	0.00328	0.00281	0.00195
−10	0.00761	0.00776	0.00823	0.00838	0.00848	0.00853	0.00845	0.00812	0.00770	0.00713	0.00586	0.00469	0.00289
−8	0.01166	0.01237	0.01320	0.01373	0.01391	0.01378	0.01345	0.01247	0.01129	0.01003	0.00784	0.00600	0.00345
−6	0.01940	0.02142	0.02303	0.02380	0.02363	0.02291	0.02189	0.01955	0.01747	0.01484	0.01034	0.00750	0.00400
−5	0.02854	0.03191	0.03457	0.03535	0.03437	0.03244	0.03017	0.02535	0.02082	0.01777	0.01190	0.00823	0.00426
−4	0.03889	0.04907	0.05390	0.05412	0.05126	0.04768	0.04341	0.03368	0.02596	0.02052	0.01349	0.00891	0.00448
−3	0.06865	0.08980	0.09624	0.09053	0.08126	0.07060	0.06075	0.04472	0.03219	0.02381	0.01494	0.00953	0.00467
−2.5	0.09546	0.13192	0.13653	0.12343	0.10503	0.08744	0.07240	0.05054	0.03546	0.02550	0.01563	0.00980	0.00475
−2	0.14401	0.21104	0.20418	0.17125	0.13708	0.10835	0.08569	0.05629	0.03861	0.02710	0.01624	0.01004	0.00482
−1.5	0.24112	0.37092	0.32142	0.24374	0.17851	0.13189	0.09976	0.06159	0.04147	0.02850	0.01676	0.01024	0.00487
−1	0.55624	0.80415	0.53274	0.34051	0.22575	0.15594	0.11298	0.06616	0.04381	0.02961	0.01717	0.01040	0.00491
−0.5	-	2.11369	0.88126	0.43917	0.26667	0.17442	0.12258	0.06925	0.04520	0.03032	0.01745	0.01051	0.00494
0	-	4.19745	1.11300	0.48698	0.28456	0.18184	0.12603	0.07036	0.04558	0.03060	0.01758	0.01057	0.00495
0.5	3.25885	2.12779	0.87756	0.43877	0.26678	0.17458	0.12268	0.06922	0.04518	0.03031	0.01745	0.01050	0.00494
1	0.70452	0.80885	0.53111	0.33897	0.22496	0.15561	0.11284	0.06615	0.04378	0.02959	0.01718	0.01037	0.00491
1.5	0.30697	0.37162	0.32199	0.24401	0.17771	0.13151	0.09947	0.06162	0.04147	0.02854	0.01677	0.01020	0.00488
2	0.17997	0.21304	0.20484	0.17190	0.13688	0.10766	0.08516	0.05607	0.03862	0.02721	0.01631	0.01001	0.00482
2.5	0.11725	0.13445	0.13637	0.12393	0.10522	0.08709	0.07174	0.05031	0.03538	0.02557	0.01574	0.00980	0.00476
3	0.08295	0.09255	0.09603	0.09097	0.08144	0.07049	0.06047	0.04474	0.03206	0.02378	0.01507	0.00955	0.00468
4	0.04828	0.05204	0.05419	0.05398	0.05146	0.04783	0.04335	0.03366	0.02594	0.02046	0.01349	0.00893	0.00449
5	0.03433	0.03376	0.03536	0.03535	0.03434	0.03250	0.03033	0.02530	0.02077	0.01779	0.01188	0.00821	0.00426
6	0.02229	0.02279	0.02351	0.02394	0.02374	0.02293	0.02185	0.01954	0.01749	0.01485	0.01033	0.00747	0.00400
8	0.01410	0.01322	0.01364	0.01389	0.01398	0.01383	0.01351	0.01248	0.01130	0.01000	0.00784	0.00598	0.00345
10	0.00859	0.00820	0.00834	0.00841	0.00850	0.00854	0.00846	0.00813	0.00767	0.00716	0.00589	0.00470	0.00289
14	0.00402	0.00405	0.00407	0.00408	0.00408	0.00409	0.00409	0.00404	0.00389	0.00370	0.00328	0.00281	0.00194

distribution is debated.[9] This article suggested that TG-43 method can be replaced with dose rate tables, but it also indicates advantages of TG-43 formalism versus dose rate table method. Actually, dose rate tables are produced from multiplying TG-43 parameters such as dose rate constant, geometry factor, anisotropy function, and radial dose function. Eventually, a normalized dose rate table with the dose rate constant can be better and simpler from TG-43 protocol in dose calculation for common brachytherapy sources. Although that article has discussed advantages and disadvantages of TG-43 dose calculation formalism versus direct calculation of dose rate table, it lacks a quantitative comparison of the results of these two methods. In the present study, the numerical results by these two methods were compared and discussed.

Calculation of three-dimensional dose distribution around brachytherapy sources may be possible by extension of two-dimensional dose distribution from the matrix-based method. For this purpose, rotation of the data around the source's longitudinal axis may be useful. In general, it can be mentioned that the current matrix-based method does not eliminate the defects (such as ignoring inhomogeneities, etc.) which are related to the TG-43 formalism. To account for such situations, some modifications on the matrix-based method are essential. As examples of such modifications, multiplication by appropriate attenuation factors, superimposition, etc., can be mentioned and these would be as participants for the future studies on this method.

CONCLUSION

According to the results obtained from these two methods, it can be concluded that the matrix-based method can be used to obtain dose distribution around various photon-emitting brachytherapy sources without performing complex calculations and through an easier way. However, TG-43 method can be used for accurate assessment of a brachytherapy source comparing with other sources regarding differences between sources' strength, radial variation of dose in the transverse plane and anisotropy of dose distributions around the sources. Therefore, due to the ease of calculations in the matrix-based method a well as due to eliminating the possible uncertainties related to independent calculation of each of the TG-43 parameters and their combined uncertainties, it is proposed that two-dimensional dose distributions from the matrix-based method be introduced into brachytherapy treatment planning systems.

The results of comparison of matrix-based method and TG-43 method for calculating two-dimensional dose distribution around the brachytherapy sources in this study showed that the dose distributions obtained from these two methods have good agreement with each other in most of data points. However, minor differences were also observed between the two methods in some points, especially for points that are further from the source. According to Table 10, mean differences for the ^{60}Co, ^{137}Cs, ^{192}Ir, and ^{103}Pd sources are 1.4%, 3.52%, 2.67%, and 2.42%, respectively. It seems that this difference is due to uncertainty in calculation of each of TG-43 parameters and their combinational uncertainties.

The dose distribution in the matrix-based approach compared to the TG-43 method is calculated with more ease and less time. However, the advantage of the TG-43 method is that it is more useful for comparing brachytherapy sources because this method shows source's strength, radial variation of dose in the transverse plane, and anisotropy of source more precise than the matrix-based method.

Table 8: Two-dimensional dose distribution per air kerma strength (cGy/h/U) for ^{103}Pd source obtained from the matrix-based method

Z (cm)	*Y* (cm)					
	0	1	2	3	4	5
0	-	0.7096	0.1085	0.0276	0.0088	0.0032
1	0.6085	0.3021	0.0768	0.0228	0.0078	0.0027
2	0.0826	0.0714	0.0349	0.0136	0.0053	0.0020
3	0.0207	0.0194	0.0131	0.0069	0.0032	0.0014
4	0.0066	0.0062	0.0049	0.0031	0.0017	0.0009
5	0.0023	0.0023	0.0018	0.0014	0.0008	0.0004

Table 9: Two-dimensional dose distribution per air kerma strength (cGy/h/U) for ^{103}Pd source obtained from the task group number-43 method

Z (cm)	*Y* (cm)					
	0	1	2	3	4	5
0		0.7070	0.1086	0.0279	0.0088	0.0031
1	0.6080	0.3051	0.0789	0.0234	0.0078	-
2	0.0822	0.0733	0.0357	0.0142	0.0056	-
3	0.0211	0.0199	0.0138	0.0070	0.0031	-
4	0.0064	0.0064	0.0051	0.0031	-	-
5	0.0022	-	-	-	-	-

Table 10: The percentage difference between results of two-dimensional dose distribution for the ^{60}Co, ^{137}Cs, ^{192}Ir, and ^{103}Pd sources from the matrix-based method and the task group number-43 method

	Mean difference (%)	Range of variation of difference (%)
^{60}Co	1.4	0.01-8.85
^{137}Cs	3.52	0.06-10.18
^{192}Ir	2.67	0.02-26.06
^{103}Pd	2.42	0.01-5.03

Finally, considering that in calculations of treatment planning systems, comparison of brachytherapy sources is not essential and also considering the more uncertainty in the calculation of dose distribution by TG-43 method, it is recommended that dose distribution obtained from matrix-based method be used as input for treatment planning systems. Extension of the matrix-based method can be a subject for further studies in this field.

Financial support and sponsorship

Nil.

Conflicts of interest

There are no conflicts of interest.

REFERENCES

1. Khan FM. The Physics of Radiation Therapy. Philadelphia, Pennsylvania, United States: Lippincott Williams and Wilkins; 2010.
2. Rivard MJ, Butler WM, DeWerd LA, Huq MS, Ibbott GS, Meigooni AS, *et al.* Supplement to the 2004 update of the AAPM Task Group No. 43

Report. Med Phys 2007;34:2187-205.
3. Bernard S, Vynckier S. Dosimetric study of a new polymer encapsulated palladium-103 seed. Phys Med Biol 2005;50:1493-504.
4. Mowlavi A, Binesh A, Moslehitabar H. Dose distribution and dosimetry parameters calculation of MED3633 ^{103}Pd source in water phantom using MCNP. Iran J Radiat Res 2006;4:15-20.
5. Pérez-Calatayud J, Granero D, Ballester F, Puchades V, Casal E. Monte Carlo dosimetric characterization of the Cs-137 selectron/LDR source: Evaluation of applicator attenuation and superposition approximation effects. Med Phys 2004;31:493-9.
6. Slate LJ, Elson HR, Lamba MA, Kassing WM, Soldano M, Barrett WL, *et al.* A Monte Carlo brachytherapy study for dose distribution prediction in an inhomogeneous medium. Med Dosim 2004;29:271-8.
7. Taylor RE, Yegin G, Rogers DW. Benchmarking brachydose: Voxel based EGSnrc Monte Carlo calculations of TG-43 dosimetry parameters. Med Phys 2007;34:445-57.
8. Zehtabian M, Faghihi R, Sina S. A review on main defects of TG-43. Brachytherapy. London, United Kingdom: InTech; 2012.
9. Song H, Luxton G, Hendee WR. Calculation of brachytherapy doses does not need TG-43 factorization. Med Phys 2003;30:997-9.
10. Granero D, Pérez-Calatayud J, Ballester F. Technical note: Dosimetric study of a new Co-60 source used in brachytherapy. Med Phys 2007;34:3485-8.
11. Meigooni AS, Wright C, Koona RA, Awan SB, Granero D, Perez-Calatayud J, *et al.* TG-43 U1 based dosimetric characterization of model 67-6520 Cs-137 brachytherapy source. Med Phys 2009;36:4711-9.
12. Granero D, Pérez-Calatayud J, Ballester F. Monte Carlo calculation of the TG-43 dosimetric parameters of a new BEBIG Ir-192 HDR source. Radiother Oncol 2005;76:79-85.
13. Mozaffari A, Ghorbani M. Determination of TG-43 dosimetric parameters for photon emitting brachytherapy sources. J Biomed Phys Eng 2017; Online First. Available from: http://www.jbpe.org/Journal_OJS/JBPE/index.php/jbpe/article/view/570/0. [Last accessed on 2018 Jul 22].